Analytica Chimica Acta 651 (2009) 42–47

Contents lists available at ScienceDirect

Analytica Chimica Acta

journal homepage: www.elsevier.com/locate/aca

Sensitive DNA biosensor improved by Luteolin copper(II) as indicator based on silver nanoparticles and carbon nanotubes modified electrode

Shuyan Niu, Bin Han, Wei Cao, Shusheng Zhang*

Key Laboratory of Eco-chemical Engineering, Ministry of Education; College of Chemistry and Molecular Engineering, Qingdao University of Science and Technology, Qingdao 266042, PR China

ARTICLE INFO

Article history:
Received 19 May 2009
Received in revised form 30 July 2009
Accepted 11 August 2009
Available online 18 August 2009

Keywords:
Luteolin copper
Carbon nanotube
4-Aminobenzoic acid
Silver nanoparticles
Electrochemical DNA biosensor

ABSTRACT

A novel and sensitive electrochemical DNA biosensor has been developed for the detection of DNA hybridization. The biosensor was proposed by using copper(II) complex of Luteolin $C_{30}H_{18}CuO_{12}$ (CuL_2) as an electroactive indicator based on silver nanoparticles and multi-walled carbon nanotubes (Ag/MWCNTs) modified glassy carbon electrode (GCE). In this method, the 4-aminobenzoic acid (4-ABA) and Ag nanoparticles were covalently grafted on MWCNTs to form Ag/4-ABA/MWCNTs. The proposed method dramatically increased DNA attachment quantity and complementary ssDNA detection sensitivity for its large surface area and good charge-transport characteristics. DNA hybridization detection was performed using CuL_2 as an electroactive indicator. The CuL_2 was synthesized and characterized using elemental analysis (EA) and IR spectroscopy. Cyclic voltammetry (CV) and fluorescence spectroscopy were used to investigate the interaction between CuL_2 and ds-oligonucleotides (dsDNA). It was revealed that CuL_2 presented high electrochemical activity on GCE, and it could be intercalated into the double helices of dsDNA. The target ssDNA of the human hepatitis B virus (HBV) was quantified in a linear range from 3.23×10^{-12} to 5.31×10^{-9} M ($r = 0.9983$). A detection limit of 6.46×10^{-13} M (3σ, $n = 11$) was achieved.

© 2009 Elsevier B.V. All rights reserved.

1. Introduction

The detection of DNA hybridization is of central importance for its application in diagnosis of pathogenic and genetic diseases [1–3]. Because of its intrinsic specificity, the hybridization between complementary ssDNA chains has been used as a bio-recognition event in the design of a great number of DNA biosensors. This recognition event can be detected using different methods, such as electrochemical [4,5], surface plasmon resonance spectroscopy [6] and electrochemiluminescence [7]. Electrochemical DNA biosensors are attractive devices for their abilities of converting DNA hybridization event into an analytical electronic signal to obtain sequence-specific information, and are applied in clinical, environmental or forensic investigations [8].

DNA immobilization at an electrode surface plays an important role in the performance of DNA biosensors. Several methods have been used to anchor DNA strands, such as direct covalent binding [9], adsorption, polymer film [10] or via the avidin–biotin affinity system [11]. Recently, carbon nanotube (CNT)-modified electrodes have attracted considerable attention in DNA sensing, which could drastically improve the effective surface area of the electrodes, heterogeneous electron transfer and long-range electron transfer [12–14]. CNT can be functionalized to achieve improved properties and functions, such as good biocompatibility and biomolecular recognition capabilities. Especially, MWCNTs loaded nanoparticles could further enhance the sensitivity of electrochemical DNA biosensor. Thus, many different schemes for electrochemical DNA sensing based on MWCNTs have been reported [13,15–17].

DNA hybridization biosensors can be exploited for monitoring sequence-specific hybridization events directly based on the oxidation signal of guanine/adenine or using DNA intercalators [18–20]. Many kinds of indicators with different sensitivity and electroactivity have been developed for the hybridization detection, such as anticancer agents [21], organic dyes [22,23], metal complex [24,25]. DNA hybridization indicators based on Os(II/III), Ru(II), Mn(II) and Cu(II) complexes with 1,10-phenanthroline or 2,2′-bipyridine have been reported due to their high sensitivity and selectivity [26–30]. In our laboratory, many efforts were also conducted to explore the interaction between DNA and ligands complex [31,32]. To the best of our knowledge, using Luteolin(2-(3,4-dihydroxyphenyl)-5,7-dihydroxy-4H-l-benzopyran -4-one) ligand coordinated to metal

Abbreviations: 4-ABA, 4-aminobenzoic acid; B–R buffer, Britton–Robinson buffer; CV, cyclic voltammetry; DPV, differential pulse voltammetry; EA, elemental analysis; EIS, electrochemical impedance spectroscopy; GCE, glassy carbon electrode; HBV, human hepatitis B virus; MWCNTs, multi-walled carbon nanotubes.

* Corresponding author. Tel.: +86 532 84022750; fax: +86 532 84022750.
E-mail address: shushzhang@126.com (S. Zhang).

0003-2670/$ – see front matter © 2009 Elsevier B.V. All rights reserved.
doi:10.1016/j.aca.2009.08.002

forming Luteolin complex as a interaction indicator has not been reported.

Luteolin is a flavonoid, which demonstrates a wide range of biochemical and pharmacological effects, including antioxidation, antiinflammation, antiplatelet, antithrombotic action, and antiallergic effects [33–35]. Recent studies have also shown that it could enter the cellular nuclei and suppress the oxidative damage of DNA [19]. Hirano and co-workers reported that Luteolin inhibited phosphorylation of c-Jun and DNA binding activity of AP-1 in nuclear lysates from stimulated KU812 cells [20]. On the other hand, Luteolin as a phenolic compound could act as a metal-chelating agent due to the functional sites of the 3′OH and 4′OH as well as 5OH and 4C=O groups in the molecule. The Luteolin complex was considered to have a better biological activity due to its cooperative effectiveness in the coordination chemistry.

In the present paper, Luteolin was chosen as a ligand for the synthesis of copper(II) complex(CuL_2) and was first used as a new electroactive indicator. The interaction between the CuL_2 and dsDNA was investigated by CV and fluorescence spectroscopy methods. The experimental results show that CuL_2 could bind with dsDNA to form a complex mainly by intercalation. The sensitivity of this electrochemical DNA biosensor for the hybridization detection was improved based on Ag/4-ABA/MWCNTs.

2. Experimental

2.1. Reagents

MWCNTs (with a diameter of about 40–60 nm and length of around 1–10 μm) with carboxylic groups were obtained from Shenzhen Nanotech Co. Ltd. (Shenzhen, China). All of the oligonucleotides related to HBV gene were supplied (as lyophilized powder) from SBS Genetech Company (Beijing, China). Their base sequences are as below:

- DNA probe (21-mer base sequence S_1): 5′-SH-AAT GTG CTC CCC CAA CTC CTC-3′.
- Target DNA (21-mer base sequence S_2): 5′-GAG GAG TTG GGG GAG CAC ATT-3′.
- non-complementary to S_1 (21-mer base sequence S_3): 5′-AAA AGG TGT AAG CGT TTG CCG-3′.
- One base mismatch to S_1 (21-mer base sequence S_4): 5′-GAG GAG TTG GGG GAG CAG ATT-3′.
- Three base mismatch to S_1 (21-mer base sequence S_5): 5′-GAC GAG TTG CGG GAG CTC ATT-3′.

All oligonucleotide stock solutions were prepared in TE solution (10 mM Tris–HCl plus 1 mM EDTA, at pH 8.0) and kept frozen. Other chemicals employed were all of analytical grade and ultrapure water was used throughout.

2.2. Instrumentation

The IR spectra were recorded on a Nicolet 510P FT-IR spectrometer (Nicolet, USA) in the wave number range of 400–4000 cm^{-1} using KBr sheets. EA was performed on Elementar Vario EL III analyzer. All electrochemical measurements, including CV, differential pulse voltammetry (DPV) and electrochemical impedance spectroscopy (EIS), were carried out with Model CHI 832B and CHI 660C electrochemical analyzers (CH Instruments, USA). A three-electrode system was employed, including Pt wire as the auxiliary electrode, Ag/AgCl as the reference electrode and GCE as the working electrode. Spectroscopic experiments were conducted on Hitachi F-4500 fluorescence spectrometer (Japan).

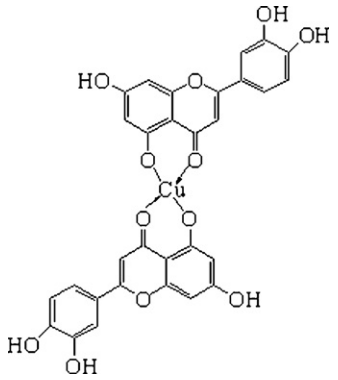

Scheme 1. The molecular structure of CuL_2.

2.3. Preparation of CuL_2

The complex CuL_2 (Scheme 1) was synthesized as described in the literature [36] and dihydroxybenzene was protected first by boracic acid. Elementary analysis: Calc. (Found) for $C_{30}H_{18}CuO_{12}$: C 54.83 (55.03); H 2.51(2.66) %. IR (cm^{-1}, m, middle; s, strong; vs, very strong): 3409vs (–OH), 1636s (C=O), 1588s, 1533m (benzene ring skeleton C=C), 1255s (C–O and OH in plane), 1167s, 1125s (C–O–C), 637m (Cu–O).

2.4. Preparation of the electrochemical DNA biosensor

2.4.1. Preparation of Ag nanoparticles and MWCNTs on GCE surface

The immobilization of MWCNTs on GCE was conducted as follows: the GCE was first polished successively with 1.0, 0.3 and 0.05 μm α-Al_2O_3 suspension. Afterwards, 5 μL of 5 M suspension of MWCNTs was dropped onto a freshly smoothed GCE surface uniformly, and the solvent was then evaporated under an infrared lamp.

The electrochemical synthesis of Ag nanoparticles on the MWCNTs surface was shown in Fig. 1. It is a three-step process analogous to the procedure employed to synthesis Ag nanoparticles on carbon nanotubes [37]: (1) the MWCNTs modified GCE was first immersed into an 0.1 M KCl solution containing 7.0 mM 4-ABA at a scan rate of 10 mV s^{-1} in a potential from 0.4 to 1.4 V (vs SCE), (2) the 4-ABA monolayer-grafted MWCNTs electrode was then immersed into 1 mM $Ag(NH_3)_2^+$ solution for 3 min and (3) after rinsing thoroughly with KNO_3 solution, the $Ag(NH_3)_2^+$ adsorbed MWCNTs electrode was transferred into 0.1 M KNO_3 solution and Ag nanoparticles were grown on the 4-ABA monolayer-grafted MWCNTs electrode by a chronoamperometry method. The potential was stepped from 0.0 to 0.5 V (vs SCE) for 120 ms.

2.4.2. ssDNA covalently immobilized to the Ag/MWCNTs modified GCE surface

The Ag/MWCNTs modified electrode was incubated in a 2.25×10^{-5} mM oligonucleotides/acetate buffer solution for 12 h at room temperature. In this process the probe oligonucleotides were immobilized on the GCE.

2.4.3. Hybridization reaction

Hybridization reaction was carried out by immersing the ssDNA probe captured Ag/MWCNTs/GCE into a stirred hybridization solution (0.2 M BR buffer) containing different concentration of DNA target for 40 min at 40 °C. After that, the electrode was rinsed three times with a 0.2% SDS phosphate buffer (pH 7.3) to remove the non-hybridized target DNA.

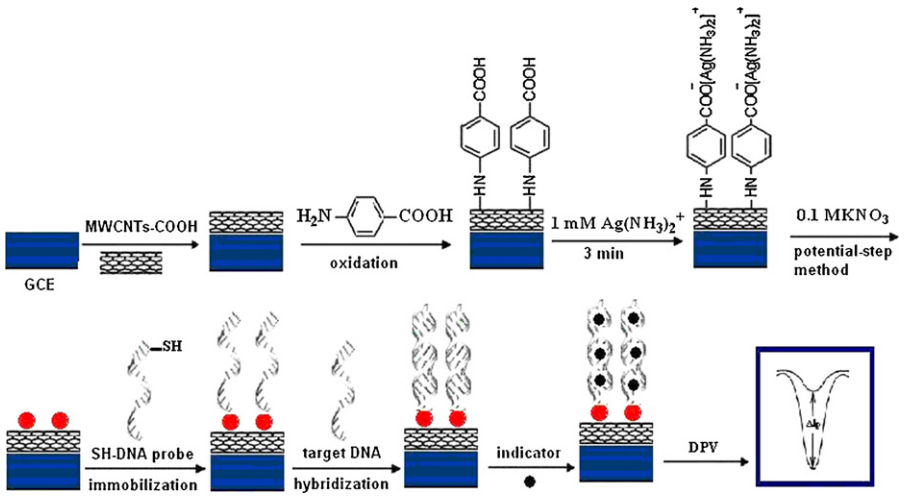

Fig. 1. Procedure for the preparation of Ag/MWCNT-modified GCE and immobilization and detection of DNA.

2.5. Binding of hybridization indicator

The binding of CuL_2 on the ssDNA immobilized or dsDNA immobilized electrode was performed as follows: the electrode was immersed in 0.20 M BR buffer solution (pH 5.0) containing 1.0×10^{-4} M CuL_2 for 10 min at room temperature. Then, the electrode was washed with ultrapure water to remove the remnant CuL_2 on the electrode surface.

2.6. Electrochemical behavior of the interaction between MnL and dsDNA

The electrochemical investigation of hybridization was carried out using DPV measurements in a 0.2 M BR buffer (pH 5.0), in a potential scanning range from −0.1 to 0.2 V (vs Ag/AgCl). The peak current related to the oxidation of CuL_2 at approximately +0.05 V was adopted as the detection signal.

The procedure of the preparation and operation of the sensor, including the modification of MWCNTs, immobilization, hybridization and detection of DNA, was illustrated in Fig. 1.

3. Results and discussion

3.1. Interaction between CuL_2 and ds DNA in solutions

3.1.1. Cyclic voltammetry study of the interaction between dsDNA and CuL_2

Cyclic voltammetry was employed to explore the interaction between CuL_2 and dsDNA. Cyclic voltammograms (Fig. 2) were obtained at 25 °C on bare GCE, in a 0.2 M BR buffer (pH 5.0) containing 6.00×10^{-5} M CuL_2, without dsDNA (curve a) and containing dsDNA of various concentrations (curves b–d), respectively. A couple of non-reversible redox peaks for CuL_2 was found. The peak current was decreased and the formal potential ($E^{\circ\prime}$) was shifted positively with the increased concentration of dsDNA and the shifts (2.0–1.0 mV and 1.0–21.0 mV) were observed when dsDNA reached a concentration of 5.18×10^{-7} M. No significant change in peak current and potential was observed when ssDNA was added in solution in the control experiment. This demonstrated the occurrence of the interaction between dsDNA and CuL_2.

The discrimination of binding modes between small molecules and DNA had been reported by Bard and co-workers previously [38]. If the formal potential ($E^{\circ\prime}$) shifted to more negative value, the interaction mode was electrostatic binding. On the contrary, if $E^{\circ\prime}$ shifted to more positive value, the interaction mode was intercalative binding. Therefore, the interaction between CuL_2 and dsDNA was attributed to the intercalative binding in this study. It was generally accepted that the planar aromatic heterocycle in Luteolin played a major intercalation role and inserted in the double helix of ds-oligonucleotides. Moreover, the decrease of peak current was also observed with the increasing concentration of dsDNA (as far as the peak current of anodic peak (I_{pa}) is concerned, the value of variational peak current is linear proportion to the logarithmic concentration of ds-oligonucleotides in the range of 1.78×10^{-7} to 1.51×10^{-6} M, following equation below: $\Delta I_{pa} = 5.93 \times 10^{-5}\,A + [8.57 \times 10^{-6} \lg C_{DNA}/(\mathrm{mol\,L^{-1}})]\,A$.

3.1.2. Optimization of experimental parameters

The influence of experimental conditions, including the pH of B–R buffer and the reaction time, were explored for optimum analytical performance. pH 5.0 was chosen because the maximum peak current change (before and after addition of dsDNA) was obtained. After incubation of 10 min the peak current reached a constant value, therefore, 10 min was chosen as the reaction time. The peak current of anodic peak (I_{pa}) was directly proportional to the square root of scan rates ranging from 0.02 to 0.30 V s^{-1} (shown in Fig. 3),

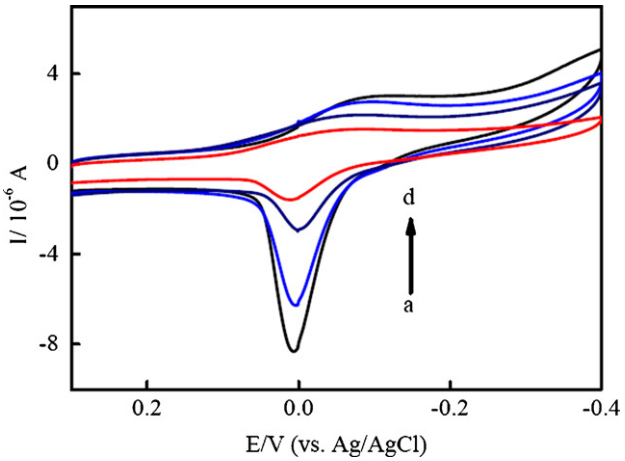

Fig. 2. Cyclic voltammograms of CuL_2 in the absence and presence of dsDNA: (a) 6.00×10^{-5} M CuL_2; (b) 6.00×10^{-5} M CuL_2 and 1.76×10^{-7} M dsDNA; (c) 6.00×10^{-5} M CuL_2 and 3.49×10^{-7} M dsDNA; (d) 6.00×10^{-5} M CuL_2 and 5.18×10^{-7} M dsDNA, respectively. Scan rate: 0.1 V s^{-1}; the potential scan: 0.3 to −0.4 V at (vs Ag/AgCl).

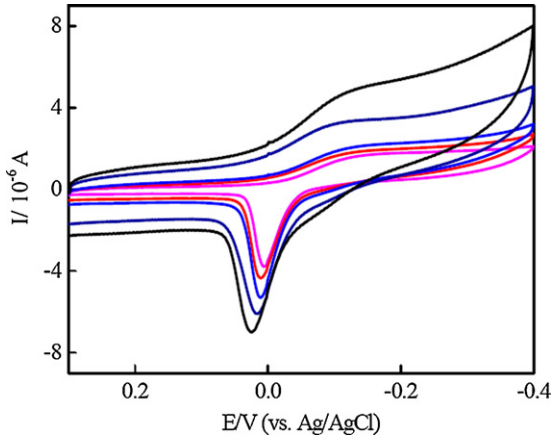

Fig. 3. Cyclic voltammograms curves of CuL_2 in the different scan rates range from 0.02 to 0.30 V s^{-1}.

indicating that the electro-oxidation process of CuL_2 was diffusion-controlled.

3.2. Fluorescence spectroscopic study of the interaction between CuL_2 and dsDNA

To further investigate the possible intercalative binding of CuL_2 complex with DNA, the fluorescence spectra (Fig. 4) of EB-dsDNA system containing different amounts of CuL_2 were also studied. As shown in Fig. 4, EB itself emitted relatively weak fluorescence emission (curve d, fluorescence intensity 71.3), but a significant increase of EB fluorescence intensity was observed (curve a, fluorescence intensity 113.5) after it intercalated into the double helix of DNA molecule. Curves b and c showed the quenching fluorescence for EB-DNA system after different amounts of CuL_2 was added (fluorescence intensities 95.7 and 81.8, respectively). Commonly, intercalation mode of CuL_2 with DNA is usually based on $C_M/C_{DNA} < 100$. Fluorescence value decreased 50% are used as a criterion of intercalation mode of compound with DNA [39]. The result demonstrated that CuL_2 and EB compete for the same binding sites of DNA and weaken the fluorescence intensity of EB-DNA system, which further confirmed the intercalation mode of CuL_2 with DNA. It is concluded that the CuL_2 could enter the interior of DNA molecule and intercalate into the base pairs of DNA as the EB.

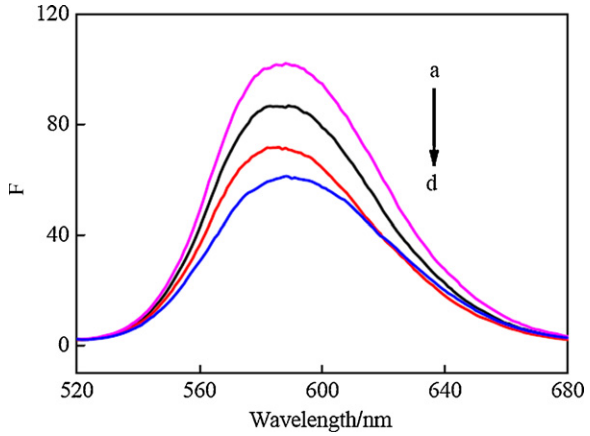

Fig. 4. Fluorescence spectra of EB–DNA system in the absence and presence of CuL_2. λ_{ex} = 520 nm; C_{DNA}, 6.64×10^{-5} M; C_{EB}, 2.45×10^{-5} M. (a) EB + DNA; (b) EB + DNA + 1.00×10^{-5} M CuL_2; (c) EB + DNA + 2.00×10^{-5} M CuL_2; (d) EB.

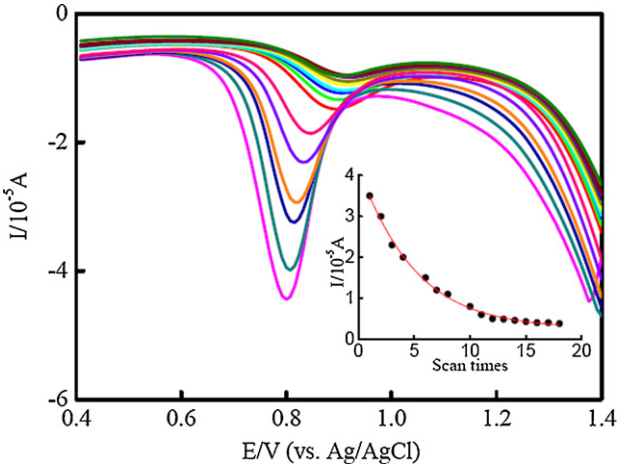

Fig. 5. Differential pulse voltammograms on a glassy carbon electrode in 0.1 M KCl with 7.0 mM 4-ABA for 18 times. Inset: peak currents vs scan times.

3.3. Covalent modification of MWCNTs with 4-ABA

Fig. 5 shows differential pulse voltammograms of 7.0 mM 4-ABA in 0.1 M KCl solution on a MWCNTs modified GCE. Then 4-ABA was found to oxidize at about 0.80 V. This oxidation wave is attributed to one-electron oxidation of the amino group to its cation radical [40]. Inset in Fig. 5 shows the peak currents vs scan times. When the potential is repeatedly scanned, the peak diminishes and almost becomes a constant after 12 times. It was indicated the formation of a 4-ABA monolayer on the electrode surface.

3.4. Electrochemical characteristics of Ag/MWCNTs/GCE

The electrochemical probe molecule $Fe(CN)_6^{3-}/Fe(CN)_6^{4-}$ was chosen to characterize the different modified electrodes. As shown in Fig. 6, curve a is the CV response of GCE in a solution of 0.10 M KCl containing 5 mM $Fe(CN)_6^{3-/4-}$, curve b is that of MWCNTs/GCE, curve c is that of 4-ABA/MWCNTs/GCE and inset is that of Ag_{nano}/MWCNTs/GCE. Compared with the GCE (Fig. 6a) and MWCNTs/GCE (Fig. 6b), the back current of 4-ABA/MWCNTs/GCE (Fig. 6c) is the largest. This shows that the effective electrode surface of 4-ABA/MWCNTs/GCE is larger than that of GCE or MWCNTs modified GCE alone. Fig. 6 inset exhibits a similar back

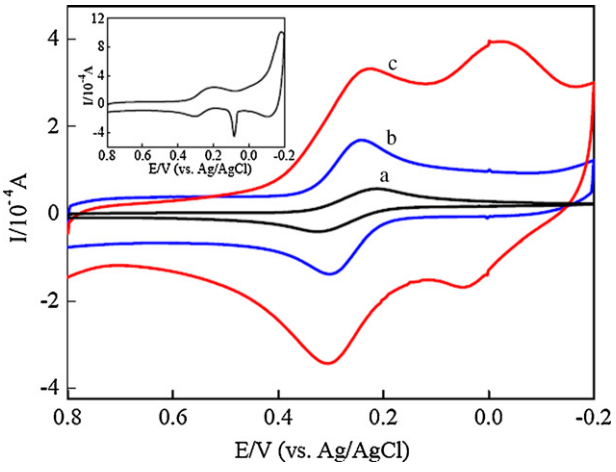

Fig. 6. Cyclic voltammograms of GCE (curve a), MWCNTs/GCE (curve b), 4-ABA/MWCNTs/GCE (curve c) and Ag/MWCNTs/GCE(inset) recorded in a solution of 0.10 M KCl containing 5 mM $Fe(CN)_6^{3-/4-}$. Scan rate 0.05 V s^{-1}; scan range +0.8 to −0.20 V.

current like curve c and an anodic peak of Ag at the potential of 0.1 V, which clearly shows that $Ag(NH_3)_2^+$ has been coordinated and reduced on the 4-ABA mono-layer-grafted MWCNTs surfaces. The GCE modified by MWCNTs and Ag_{nano} (Fig. 6 inset) exhibits the highest electroactive surface area according to the Randles–Sevcik equation [41]. $I_p = 2.69 \times 10^5 AD^{1/2} n^{3/2} \gamma^{1/2} C$, where n is the number of electrons participating in the redox reaction, A is the area of the electrode (cm), D is the diffusion coefficient of the molecule in solution ($cm^2\ s^{-1}$), C is the concentration of the probe molecule in the bulk solution ($mol\ cm^{-3}$), and γ is the scan rate of the potential perturbation ($V\ s^{-1}$). For the MWCNTs modified GCE, the peak current is still pronounced (Fig. 6b) than that of the bare GCE (Fig. 6a), but it exhibits a decrease compared with that of 4-ABA/MWCNTs/GCE and Ag/MWCNTs/GCE, likely due to the lack of Ag nanoparticles or 4-ABA that were in contact with MWCNTs. With MWCNTs and Ag_{nano} having a much larger surface area, the quantities of ssDNA immobilized on the electrode surface can greatly enhanced, therefore the detection limits of sequence-specific DNA in solution should be greatly lowered.

3.5. SsDNA hybridization detection using impedance spectroscopy

Electrochemical impedance spectroscopy was applied to monitor the whole procedure in the modification of the electrode. A typical EIS curve included a semicircular part and a linear part. The semicircular part obtained at higher frequency, which corresponded to the electron transfer-limited process. Its diameter was equal to the electron transfer resistance (R_{et}), which controlled the electron transfer kinetics of the redox probe on the electrode interface. The linear part obtained at lower frequency, which corresponded to the diffusion process. $Fe(CN)_6^{3-/4-}$ was chosen as the EIS probe. The EIS curves of the Ag/MWCNTs/GCE (curve a), ssDNA modified Ag/MWCNTs/GCE (curve b) and S_1–S_2 hybridized Ag/MWCNTs/GCE (curve c) obtained in a solution of 0.10 M KCl containing 10 mM $Fe(CN)_6^{3-/4-}$ and were shown in Fig. 7. When ssDNA were modified on the Ag/MWCNTs/GCE, the diameter of semicircular part greatly increased, suggesting the electron transfer of the redox probe was obstructed by ssDNA. The diameter of semicircular part in the EIS curve of S_1–S_2 hybridized Ag/MWCNTs/GCE was attributed to the low conductivity of dsDNA double helices structure. The highest electron transfer resistance slowed down the redox reaction of $Fe(CN)_6^{3-/4-}$. It was thus showed that ssDNA were immobilized on the Ag/MWCNTs/GCE surface, and target ssDNA were hybridizated with the probe ssDNA.

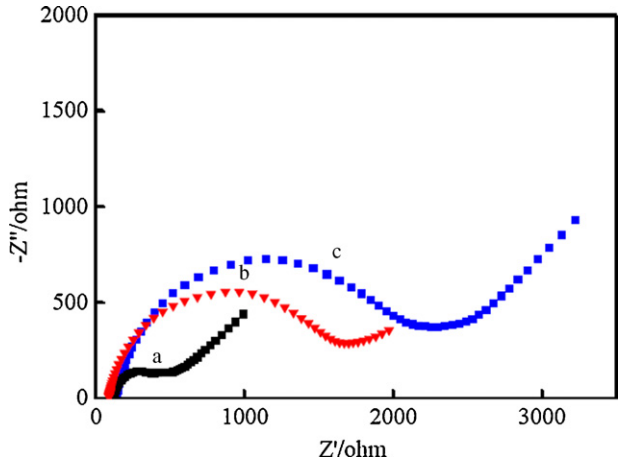

Fig. 7. Electrochemical impedance spectroscopy of modified and unmodified Ag/MWCNTs/GCE: (1) bare Ag/MWCNTs/GCEs; (2) ss-oligonucleotides modified Ag/MWCNTs/GCEs; (3) ds-oligonucleotides modified Ag/MWCNTs/GCEs.

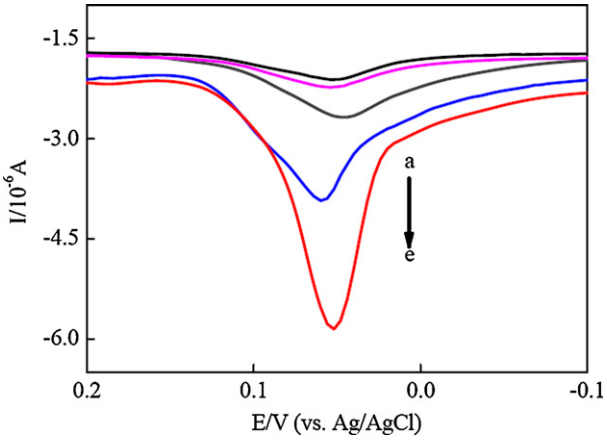

Fig. 8. DPV response of CuL_2 recorded for the oligonucleotides/Ag/MWCNTs/GCE probe: (a) without hybridization (S_1); (b) hybridized with non-complementary sequence (S_3); (c) three base mismatch sequence (S_5); (d) one base mismatch sequence (S_4); (e) complementary target DNA (S_2). The amplitude, pulse period, and pulse width were 50 mV, 0.2 s, and 50 ms, respectively. $C_{target\ DNA}$: 5.0×10^{-10} M.

3.6. Recognition by HBV DNA biosensor of its target sequence using CuL_2 as an electrochemical indicator

Based upon the above investigated, CuL_2 complex was further used as an electrochemical indicator for the detection of a synthetic 21-mer sequence of the human hepatitis B virus. The selectivity of this assay was explored by using the ssDNA/Ag/MWCNTs/GCEs to hybridize with different kinds of DNA sequence. Fig. 8 shows DPV for the signal of CuL_2 at ssDNA probe immobilized electrode (curve a), after hybridization with the non-complementary sequence (curve b), the one base mismatch sequence (S_4) (curve d), the three base mismatch sequence (S_5) (curve c) and the perfectly matched sequence (curve e).

Typically, there is only a low DPV signal of CuL_2 on the probe ssDNA modified electrode, indicating that CuL_2 has a little affinity for ssDNA on the Ag/MWCNTs/GCEs surface. A significant increase in the voltammetric signals was observed after hybridization of probe ssDNA modified electrode with the complementary HBV ssDNA. This indicates that more CuL_2 molecules are preconcentrated on the dsDNA/GCE surface due to the binding interaction between CuL_2 and immobilized HBV dsDNA. These results suggest that both the hybridization process and the target sequence of the HBV DNA fragment can be recognized using CuL_2 as an electrochemical indicator. In addition, as expected, there was no significant current difference observed before and after the non-complementary DNA sequence (S_2) was applied on ssDNA probe (S_1) modified Ag/MWCNTs/GCE, indicating that the non-specific absorption was negligible.

The sensitivity of the fabricated electrochemical DNA biosensor was studied by the different concentration of target ssDNA (S_2) complementary to the probe ssDNA (S_1) immobilized on GCE. The different anodic peak currents obtained in DPV measurement increases with the increasing concentration of S_2. The value of peak current is linear with the concentration of S_2 over the range from 3.23×10^{-12} to 5.31×10^{-9} M. The regression equation was found to be $\Delta I_{pa} = 6.37 \times 10^{-8}\ A + 1.00(C_{S2}/10^{-3}\ M)\ A$ with a correlation coefficient of 0.9983. The sample was measured by 11 parallel points, with determined RSD of 1.12%. A detection limit of 6.46×10^{-13} M for the target ssDNA was estimated using 3σ (where σ is the standard deviation of the blank solution, $n = 11$) (Fig. 9). This sensor and the related procedure would be of lower cost and more

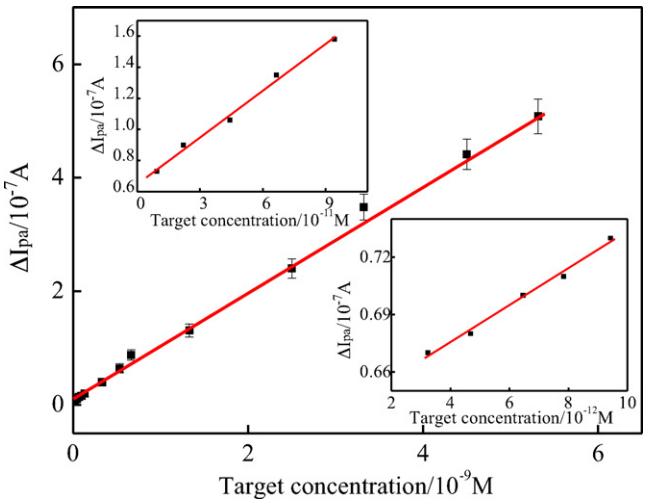

Fig. 9. The relation between concentration of target ss-oligonucleotides and anodic peak currents.

convenience compared with other methods developed for determination of HBV in the past decade [42–44], while still possess relatively high selectivity and sensitivity.

4. Conclusions

Using CuL_2 as a novel electroactive indicator, ssDNA fragment of HBV could be selectively detected on the new electrochemical DNA biosensor. Interaction between CuL_2 and dsDNA was studied by CV and fluorescence spectroscopy. It was shown that CuL_2 could be intercalated into double helices of the dsDNA. The Ag/MWCNTs were used for covalent immobilization of ssDNA probe and for the enhancement of sensitivity of sequence-specific ssDNA detection. The target HBV ssDNA could be quantified ranging from 3.23×10^{-12} to 5.31×10^{-9} M and a detection limit of 6.46×10^{-13} M.

Acknowledgement

This work was supported by the National Natural Science Foundation of China (No. 20775038), the Scientific and Technical Tackle Key Problem Project of Shandong Province (2006GG2203024), and the Scientific and Technical Development Project of Qingdao (06-3-1-4-yx).

References

[1] M.T. Castaneda, A. Merkoci, M. Pumera, S. Alegret, Biosens. Bioelectron. 22 (2007) 1961–1967.
[2] E. Palecek, F. Jelen, Crit. Rev. Anal. Chem. 32 (2002) 261–270.
[3] J. Wang, R. Polsky, A. Merkoci, K.L. Turner, Langmuir 19 (2003) 989–991.
[4] H. Karadeniz, A. Erdem, A. Caliskan, Electroanalysis 20 (2008) 1932–1938.
[5] H.Y. Ma, L.P. Zhang, Y. Pan, K.Y. Zhang, Y.Z. Zhang, Electroanalysis 20 (2008) 1220–1226.
[6] B. Nguyen, F.A. Tanious, W.D. Wilson, Methods 42 (2007) 150–161.
[7] J.G. Lee, K. Yun, G.S. Lim, S.E. Lee, S. Kim, J.K. Park, Bioelectrochemistry 70 (2007) 228–234.
[8] A. Erdem, Talanta 74 (2007) 318–325.
[9] A. Sassolas, B.D. Leca-Bouvier, L.J. Blum, Chem. Rev. 108 (2008) 109–139.
[10] Y. Xu, X.Y. Ye, L. Yang, P.G. He, Y.Z. Fang, Electroanalysis 18 (2006) 1471–1478.
[11] X.C. Zhou, L.Q. Huang, S.F.Y. Li, Biosens. Bioelectron. 16 (2001) 85–95.
[12] F. patolsky, C.M. Lieber, Mater. Today 8 (4) (2005) 20–28.
[13] A. Erdem, P. Papakonstantinou, H. Murphy, Anal. Chem. 78 (2006) 6656–6659.
[14] P. Papakonstantinou, R. Kern, L. Robinson, H. Murphy, J. Irvine, E. McAdams, J. McLaughlin, T. McNally, Fuller. Nanotub. Car. N. 13 (2005) 91.
[15] M.L. Pedano, G.A. Rivas, M.L. Pedano, Electrochem. Commun. 6 (2004) 10–16.
[16] J. Wang, G.D. Liu, M.R. Jan, J. Am. Chem. Soc. 126 (2004) 3010–3011.
[17] J. Galandova, L. Trnkova, R. Mikelova, J. Labuda, Electroanalysis 21 (2009) 563–572.
[18] A. Erdem, F. Sayar, H. Karadeniz, G. Guven, M. Ozsoz, E. Piskin, Electroanalysis 19 (2007) 798–804.
[19] K. Kazuki, U. Mari, Y. Hiroaki, H. Takashi, Arch. Biochem. Biophys. 455 (2006) 197–203.
[20] T. Hirano, S. Hig, J. Arimitsu, T. Naka, et al., Biochem. Biophys. Res. Commun. 340 (2006) 1–7.
[21] G.F. Cheng, J. Zhao, Y.H. Tu, P.A. He, Y.H. Fang, Anal. Chim. Acta 533 (2005) 11–16.
[22] V. Ostatná, N. Dolinnaya, S. Andreev, T. Oretskaya, J. Wang, T. Hianik, Bioelectrochemistry 67 (2005) 205–210.
[23] J.W. Kang, X.N. Li, G.F. Wu, Z.H. Wang, X.Q. Lu, Anal. Biochem. 364 (2007) 165–170.
[24] S.Y. Niu, M. Zhao, R. Ren, S.S. Zhang, J. Inorg. Biochem. 103 (2009) 43–49.
[25] N.C. Tansil, H. Xie, F. Xie, Z. Gao, Anal. Chem. 77 (2005) 126–134.
[26] M.V. del Pozo, C. Alonso, F. Pariente, E. Lorenzo, Anal. Chem. 77 (2005) 2550–2557.
[27] T. Garcia, M. Revenga-Parra, H.D. Abruna, F. Pariente, E. Lorenzo, Anal. Chem. 80 (2008) 77–84.
[28] Y. Ni, D. Lin, S. Kokot, Anal. Biochem. 352 (2006) 231–242.
[29] S. Dhar, M. Nethaji, A.R. Chakravarty, Inorg. Chim. Acta 358 (2005) 2437–2444.
[30] S. Dhar, D. Senapati, P.K. Das, P. Chattopadhyay, M. Nethaji, A.R. Chakravarty, J. Am. Chem. Soc. 125 (2003) 12118–12124.
[31] X.M. Li, H.Q. Ju, C.F. Ding, S.S. Zhang, Anal. Chim. Acta 582 (2007) 158–163.
[32] S.Y. Niu, S.S. Zhang, L. Wang, X.M. Li, J. Electroanal. Chem. 597 (2006) 111–118.
[33] M.T. Fernandez, M.L. Mira, M.H. Florêncio, K.R. Jennings, J. Inorg. Biochem. 92 (2002) 105–111.
[34] Middleton E.Jr.F C., Kandaswami, Biochem. Pharmacol. 43 (1992) 1167–1179.
[35] N.C. Cooks, S. Samman, J. Nutr. Biochem. 7 (1996) 66–76.
[36] Y. Bai, F.R. Song, M.L. Chen, J.P. Xing, Z.Q. Liu, S.Y. Liu, Anal. Sci. 20 (2004) 1147–1151.
[37] G.Y. Gao, D.J. Guo, C. Wang, H.L. Li, Electrochem. Commun. 9 (2007) 1582–1586.
[38] M.T. Carter, M. Rodriguez, A.J. Bard, J. Am. Chem. Soc. 111 (1989) 8901–8911.
[39] H. Grant, M. Howe-Grant, K.C. Wu, W.R. Bauer, S.J. Lippard, Biochemistry 15 (1976) 4339–4346.
[40] V. Molinero, E.J. Calvo, J. Electroanal. Chem. 445 (1998) 17–25.
[41] A.J. Bard, L.R. Faulkner, Electrochemical Methods-Fundamentals and Applications, Wiley, New York, 2000.
[42] X. Chen, X.E. Zhang, Y.Q. Chai, W.P. Hu, Z.P. Zhang, X.M. Zhang, A.E.G. Cass, Biosens. Bioelectron. 13 (1998) 451–458.
[43] S.K.N. Ho, W.C. Yam, E.T.K. Leung, L.P. Wong, J.K.H. Leung, K.N. Lai, T.M. Chan, J. Med. Microbiol. 52 (2003) 397–402.
[44] W.M. Hassen, C. Chaix, A. Abdelghani, F. Bessueille, D. Leonard, N.J. Renault, Sens. Actuators B 134 (2008) 755–760.